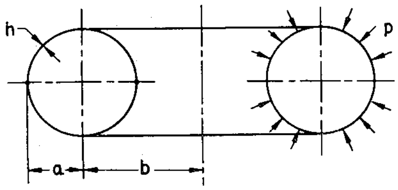

Fig. 1 Notation for a toroidal shell.

sive variations in the thickness were avoided and a high degree of accuracy in the geometry of the shell's middle surface was achieved. To obtain accurate values of the critical pressures for epoxy shells, one must select the material composition in such a way that room temperature creep is minimized. This selection results in a material that has a high modulus and is brittle. Thus when buckling occurs, the shell shatters and it is not possible to observe the development of a buckling pattern. Therefore, in addition to the shells with high modulus, one shell was manufactured from a very ductile material with a low modulus. The epoxy system for the brittle and high-modulus (E = 500,000) material is composed of 100 pbw Bakelite Resin ERL 2774, and 10 pbw Diethanolamine. The low modulus material was obtained through addition of 60 pbw Thiokol LP33 to the composition used for the brittle material. The material components were thoroughly mixed at 100°F. The mold for the half-torus together with the epoxy system was placed in a furnace that was maintained at a temperature of 160°. The epoxy was forced to fill the mold under pressure. The flow rate was held very low in order to minimize entrapment of air. About 1 hr was required to fill the mold. The male mandrel portion of the mold was allowed to free float on the resin such that it lifted when the mold was full. Then the epoxy was allowed to flow over the edges for some time before the free floating mandrel was clamped tight to the female part. After a curing cycle of 24 hr at 160°F the half-shell was removed from the mold. A room temperature curing adhesive was used to bond the two halves of the shell together. The following adhesive composition was selected to match the material properties of the shell: 100 pbw Bakelite Resin ERL 2774, 10 pbw Triethylenetetramine, 3 pbw Aluminum Powder.

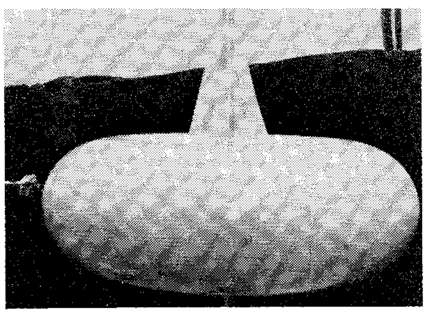

a) Unloaded shell

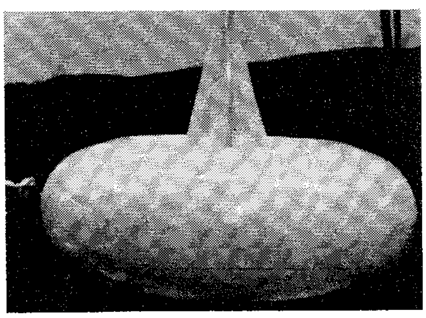

b) Axisymmetric buckling

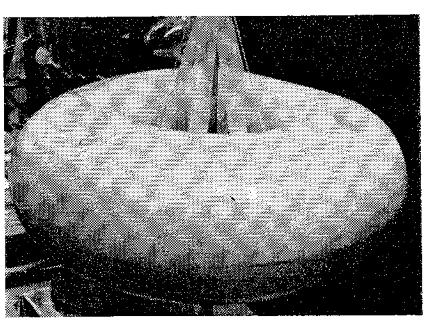

c) Nonsymmetric buckling

Fig. 2 Photographs of ductile test specimen.

Three shells made from the brittle material were tested. External pressure was applied through partial evacuation of the air in the shell. The experimentally determined pressures at failure for the shells are 6.32, 6.60, and 6.64 psi, whereas the theoretical pressure (Ref. 1) based on nominal dimensions is 7.00 psi. After the tests, thickness measurements were made on the shell fragments. It appeared that the thickness was quite uniform but somewhat less than the nominal value of 0.050 in. Thus, the experimental values are somewhat above the theoretical buckling load based on actual dimensions.

One toroidal shell was manufactured from the ductile material. The photographs in Fig. 2 show how the buckling pattern develops for this shell. Figures 2a and 2b, respectively, show the torus before and after application of pressure. From Figs. 2b, it is seen that an axisymmetric deformation pattern has developed. As the load is further increased a nonsymmetrical buckling pattern (see Fig. 2c) is superimposed on the symmetrical pattern. According to theory, the axisymmetric buckling mode is critical for a torus with b/a = 2 and a/h = 50. This buckling pattern appears to be stable (the buckle amplitude grows under increasing load). As a small amplitude symmetric buckling is difficult to detect, it seems possible that the brittle shells really buckled at loads somewhat below those at which the shell shattered. This would tend to explain the somewhat higher values of the experimental buckling pressures.

It can be concluded that for accurately manufactured toroidal shells, such as those tested here, one can expect good agreement between test and theory.

Reference

[1] Sobel, L. H. and Flügge, W., "Stability of Toroidal Shells under Uniform External Pressure," *AIAA Journal*, Vol. 5, No. 3, March 1967, pp. 425–431.

Optimized Acceleration of Convergence of an Implicit Numerical Solution of the Time-Dependent Navier-Stokes Equations

Joe F. Thompson*
Mississippi State University, State College, Miss.

Nomenclature

ζ = vorticity
ψ = stream function
ω = angular velocity of body
ν = kinematic viscosity
h = cell size
k = time step

Submitted November 15, 1968; presented as Paper 69-185 at the AIAA 7th Aerospace Sciences Meeting, New York, January 20-22, 1969; revision received July 2, 1969. This work wa supported by the U. S. Army Research Office—Durham, Project THEMIS.

* Assistant Professor, Department of Aerophysics and Aerospace Engineering.

ρ = spectral radius
T = superscript indicating matrix transpose
δ_{ij} = kroniker delta

A NUMERICAL solution of the incompressible, two-dimensional, time-dependent Navier-Stokes equations of viscous fluid motion, which is implicit in time as well as space, has been developed for the case of a uniform flow past a body with rectangular boundaries undergoing pitch oscillations.[1,2]

The method is implicit in both space and time, so that two difference equations must be solved simultaneously by iteration over the entire field at each time step. With the development of an optimized two-parameter acceleration method, it was possible to reduce the required number of iterations by more than an order of magnitude from that required by Gauss-Seidel iteration, and to remove the restriction placed on the maximum size of the time step by the Gauss-Seidel technique. The general idea of acceleration methods is, of course, well known[3]; however, the determination of the optimum acceleration parameters for, and the application to, this nonlinear set of simultaneous equations has not heretofore been given.

For two-dimensional flow, the time-dependent, incompressible Navier-Stokes equations in body-fixed coordinates may be written in terms of the vorticity ζ and the stream function ψ as

$$\frac{\partial\zeta}{\partial t} + \left(\frac{\partial\psi}{\partial y}\frac{\partial\zeta}{\partial x} - \frac{\partial\psi}{\partial x}\frac{\partial\zeta}{\partial y}\right) + 2\omega = \nu\left(\frac{\partial^2\zeta}{\partial x^2} + \frac{\partial^2\zeta}{\partial y^2}\right) \qquad (1)$$

$$\partial^2\psi/\partial x^2 + \partial^2\psi/\partial y^2 = -\zeta \qquad (2)$$

With the time derivative approximated by a three-point backward difference expression and the space derivatives approximated by central difference expressions with the intervals equal in each direction, the differential equations (1) and (2) may be approximated, respectively, by the difference equations $[\zeta_{i,j}{}^n \equiv \zeta(x_i, y_j, t_n)]$:

$$\begin{aligned}(3h^2 + 8\nu k)\zeta_{i,j}{}^n = {} & h^2(4_{i,j}{}^{n-1} - \zeta_{i,j}{}^{n-2} - 4k\dot{\omega}) + \\ & 2\nu k(\zeta_{i+1,j}{}^n + \zeta_{i-1,j}{}^n + \zeta_{i,j+1}{}^n + \zeta_{i,j-1}{}^n) - \\ & (k/2)(\psi_{i,j+1}{}^n - \psi_{i,j-1}{}^n)(\zeta_{i+1,j}{}^n - \zeta_{i-1,j}{}^n) + \\ & (k/2)(\psi_{i+1,j}{}^n - \psi_{i-1,j}{}^n)(\zeta_{i,j+1}{}^n - \zeta_{i,j-1}{}^n) \qquad (3)\end{aligned}$$

$$\psi_{i,j}{}^n = \tfrac{1}{4}(\psi_{i+1,j}{}^n + \psi_{i-1,j}{}^n + \psi_{i,j+1}{}^n + \psi_{i,j-1}{}^n) + (h^2/4)\zeta_{i,j}{}^n \qquad (4)$$

With rectangular field boundaries represented by $i = 0, I+1$, and $j = 0, J+1$, each of these difference equations represents a set of IJ equations, so that there are $2IJ$ simultaneous, algebraic equations to be solved simultaneously.

The question of stability and convergence of any iterative procedure can only be answered completely by a consideration of Eqs. (3) and (4) simultaneously, one of which equations is nonlinear. However, Poisson's equation is known to have excellent convergence properties when solved alone.[3] Therefore, it is reasonable to assume that the convergence of the simultaneous solution of the nonlinear vorticity equation (3) and the Poisson equation for the stream function (4) will be most affected by the convergence properties of the nonlinear equation. It is then reasonable that the acceleration parameters which are optimum for the vorticity equation (3) when solved alone, with $\boldsymbol{\psi}$ constant during the iteration, should also accelerate the convergence of the simultaneous solution of Eqs. (3) and (4) by a significant amount, even though the acceleration parameters so obtained would not necessarily be optimum for the simultaneous solution.

The vorticity equation (3) may be expressed in matrix† form as

$$\begin{aligned}\{(3h^2 + 8\nu k)\mathbf{I} - {} & [2\nu k\mathbf{I} + (k/2)\mathbf{M}]\mathbf{L} - [2\nu k\mathbf{I} - (k/2)\mathbf{N}]\mathbf{B} - [2\nu k\mathbf{I} - (k/2)\mathbf{M}]\mathbf{L}^T - \\ & [2\nu k\mathbf{I} + (k/2)\mathbf{N}]\mathbf{B}^T\}\boldsymbol{\zeta} = [h^2(4\boldsymbol{\zeta}^{n-1} - \boldsymbol{\zeta}^{n-2} - \\ & 4k\dot{\omega}\mathbf{I}) + 2\nu k(\mathbf{Z} + \mathbf{Y} + \mathbf{W} + \mathbf{V}) - (k/2)\mathbf{M}(\mathbf{Z} - \mathbf{Y}) + \\ & (k/2)\mathbf{N}(\mathbf{W} - \mathbf{V})] \qquad (5)\end{aligned}$$

where the matrices involved are defined as follows:

1) I-order square matrices

$$\begin{aligned}(\boldsymbol{\psi}_\mathbf{j})_{i,s} &\equiv \delta_{i,s}\psi_{i,j} & (\mathbf{Y}_\mathbf{j})_{i,s} &\equiv \delta_{i,1}\delta_{1,s}\zeta_{0,j}\\ (\boldsymbol{\zeta}_\mathbf{j})_{i,s} &\equiv \delta_{i,s}\zeta_{i,j} & (\mathbf{Z}_\mathbf{j})_{i,s} &\equiv \delta_{i,I}\delta_{I,s}\zeta_{I+1,j}\\ (\mathbf{I}_\mathbf{I})_{i,s} &\equiv \delta_{i,s} & (\mathbf{P}_\mathbf{j})_{i,s} &\equiv \delta_{i,1}\delta_{1,s}\psi_{0,j}\\ (\mathbf{L}_\mathbf{I})_{i,s} &\equiv \delta_{i-1,s} & (\mathbf{Q}_\mathbf{j})_{i,s} &\equiv \delta_{i,I}\delta_{I,s}\psi_{I+1,j}\end{aligned}$$

2) J-order square matrices with I-order square matrices for elements

$$\begin{aligned}(\boldsymbol{\psi})_{j,s} &\equiv \delta_{j,s}\boldsymbol{\psi}_\mathbf{s} & (\mathbf{L})_{j,s} &\equiv \delta_{j,s}\mathbf{L}_\mathbf{I}\\ (\boldsymbol{\zeta})_{j,s} &\equiv \delta_{j,s}\boldsymbol{\zeta}_\mathbf{s} & (\mathbf{B})_{j,s} &\equiv \delta_{j-1,s}\mathbf{I}_\mathbf{I}\\ (\mathbf{I})_{j,s} &\equiv \delta_{j,s}\mathbf{I}_\mathbf{I} & (\mathbf{Y})_{j,s} &\equiv \delta_{j,s}\mathbf{Y}_\mathbf{s}\\ (\mathbf{Z})_{j,s} &\equiv \delta_{j,s}\mathbf{Z}_\mathbf{s} & (\mathbf{V})_{j,s} &\equiv \delta_{j,1}\delta_{1,s}\boldsymbol{\zeta}_\mathbf{0}\\ (\mathbf{P})_{j,s} &\equiv \delta_{j,s}\mathbf{P}_\mathbf{s} & (\mathbf{W})_{j,s} &\equiv \delta_{j,J}\delta_{J,s}\boldsymbol{\zeta}_\mathbf{J+1}\\ (\mathbf{Q})_{j,s} &\equiv \delta_{j,s}\mathbf{Q}_\mathbf{s} & (\mathbf{R})_{j,s} &\equiv \delta_{j,1}\delta_{1,s}\boldsymbol{\psi}_\mathbf{0}\\ & & (\mathbf{S})_{j,s} &\equiv \delta_{j,J}\delta_{J,s}\boldsymbol{\psi}_\mathbf{J+1}\end{aligned}$$

Also,

$$\mathbf{M} \equiv (\mathbf{B}^T\boldsymbol{\psi}\mathbf{B} + \mathbf{S}) - (\mathbf{B}\boldsymbol{\psi}\mathbf{B}^T + \mathbf{R})$$

$$\mathbf{N} \equiv (\mathbf{L}^T\boldsymbol{\psi}\mathbf{L} + \mathbf{Q}) - (\mathbf{L}\boldsymbol{\psi}\mathbf{L}^T + \mathbf{P})$$

The vorticity equation is now in the form $\mathbf{A}\boldsymbol{\zeta} = \mathbf{F}$, in which the matrices $\mathbf{A}$ and $\mathbf{F}$ would be constant if the vorticity were being solved for alone with $\boldsymbol{\psi}$ constant during the iteration.

Let the matrix $\mathbf{A}$ be split so that $\mathbf{A} = \mathbf{A}_1 - \mathbf{A}_2$, where $\mathbf{A}_1(\sigma,\gamma) \equiv (1+\sigma)\mathbf{A}_1'(\gamma)$ with $\mathbf{A}_1'(\gamma) = (1/\gamma)(3h^2 + 8\nu k)\mathbf{I} - [2\nu k\mathbf{I} + (k/2)\mathbf{M}]\mathbf{L} - [2\nu k\mathbf{I} - (k/2)\mathbf{N}]\mathbf{B}$. Here σ and γ are the two acceleration parameters, yet to be determined.

With this splitting, Eq. (5) becomes

$$\mathbf{A}_1(\sigma,\gamma)\boldsymbol{\zeta}^{(p)} = \mathbf{A}_2(\sigma,\gamma)\boldsymbol{\zeta}^{(p-1)} + \mathbf{F} \qquad (6)$$

where the superscript indicates the iteration number. (With $\sigma = 0$ and $\gamma = 1$, this splitting represents Gauss-Seidel iteration, which always uses the most recently calculated values of ζ.) Convergence then depends on the eigenvalues of the matrix $\mathbf{D}$

$$\mathbf{D}(\sigma,\gamma) \equiv \mathbf{A}_1{}^{-1}(\sigma,\gamma)\mathbf{A}_2(\sigma,\gamma)$$

(The iterative solution converges if all the eigenvalues of $\mathbf{D}$ are less than unity in magnitude.)

For cell Reynolds number hU/ν much greater than 2, the magnitudes of the eigenvalues $\xi_{p,q}$ of $\mathbf{D}$ are given by one of the following expressions,[1] depending on the value of $a_{p,q}$. For p,q such that $a_{p,q} \geq |(1-\gamma)^{1/2}/\gamma|$, the magnitude of the corresponding eigenvalue $\xi_{p,q}$ is given by

$$|\xi_{p,q}| = \left|\frac{\sigma - \{\gamma a_{p,q} \pm [\gamma^2 a_{p,q}{}^2 - (1-\gamma)]^{1/2}\}^2}{\sigma + 1}\right| \qquad (7)$$

and for p,q such that $a_{p,q} \leq |(1-\gamma)^{1/2}/\gamma|$, the magnitude $|\xi_{p,q}|$ is given by

$$|\xi_{p,q}| = \left|\frac{[(\sigma + 1 - \gamma)^2 - 4\sigma\gamma^2 a_{p,q}{}^2]^{1/2}}{\sigma + 1}\right| \qquad (8)$$

† Matrix is indicated in bold face.

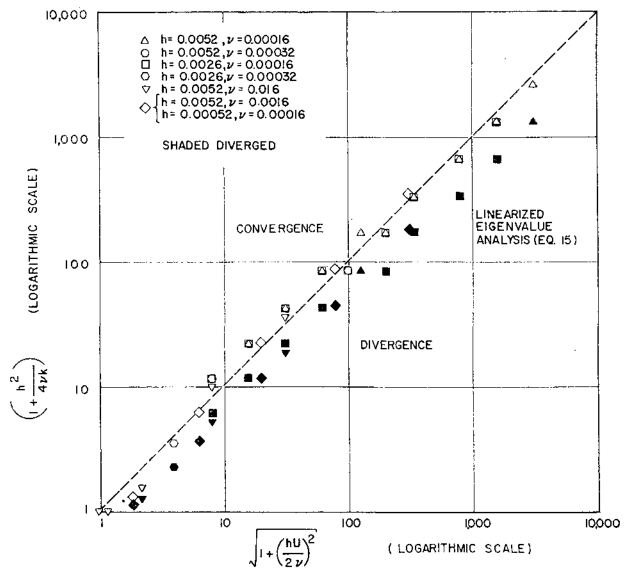

Fig. 1 Convergence properties of unaccelerated solution.

Here

$$a_{p,q} = \frac{[4 + (hU/\nu)^2]^{1/2}}{[3(h^2/\nu k) + 8]} \left[\cos\left(\frac{\pi p}{I+1}\right) + \cos\left(\frac{\pi q}{J+1}\right)\right]$$

The spectral radius of **D** then is given by

$$\rho(\sigma,\gamma) \equiv \max_{p,q} |\xi_{p,q}|$$

Maximum convergence acceleration is achieved using those values of σ and γ that minimize the spectral radius of **D**, i.e., result in the smallest maximum eigenvalue of **D** in magnitude. Now define[1]

$$(\gamma_n)_\pm \equiv (1/2a_{1,1}^2)[-1 \pm (1 + 4a_{1,1}^2)^{1/2}]$$

$$(\gamma_m)_\pm \equiv [1/2(\min_{p,q} a_{p,q})^2]\{-1 \pm [1 + 4(\min_{p,q} a_{p,q})^2]^{1/2}\}$$

Note that $\min_{p,q} a_{p,q}$ is either zero or very nearly zero so that $(\gamma_m)_+ \cong 1$, $(\gamma_m)_- \cong -\infty$.

All values of γ in the range $(\gamma_m)_- \leq \gamma \leq (\gamma_n)_-$ produce divergence ($\rho > 1$). In the range $(\gamma_n)_- \leq \gamma \leq (\gamma_m)_+$ the optimum γ and σ are $\gamma = (\gamma_n)_+$ and $\sigma = 0$, for which the spectral radius is given by

$$\rho = 1 - \{2/[1 + (1 + 4a_{1,1}^2)^{1/2}]\} \tag{9}$$

Finally, in the range $\gamma \geq (\gamma_m)_+$ the optimum γ and σ are $\gamma = 1$ and $\sigma = 2a_{1,1}^2$, with the corresponding spectral radius given by

$$\rho = 1/[1 + (1/2a_{1,1}^2)] \tag{10}$$

Since the spectral radius given by Eq. (9) is less than that given by Eq. (10), the final optimum γ and σ are

$$\sigma^* = 0 \tag{11}$$

$$\gamma^* = 2/[1 + (1 + 4a_{1,1}^2)^{1/2}] \tag{12}$$

for which the spectral radius is

$$\rho^* = 1 - \{2/[1 + (1 + 4a_{1,1}^2)^{1/2}]\} \tag{13}$$

The spectral radius of the optimized accelerated solution then is less than 1 for all values of $a_{1,1}$. This solution, therefore, converges for all values of the velocity, time step, cell size, and viscosity.

In contrast to this absolute convergence of the optimized accelerated solution, the unaccelerated solution ($\gamma = 1$, $\sigma = 0$; Gauss-Seidel iteration) is only conditionally convergent. In that case,[1]

$$\rho = \frac{4[4 + (hU/\nu)^2]}{[3(h^2/\nu k) + 8]^2} \left[\cos\left(\frac{\pi}{I+1}\right) + \cos\left(\frac{\pi}{J+1}\right)\right]^2 \tag{14}$$

so that the solution converges only if

$$[1 + (hU/2\nu)^2]/[1 + (3h^2/8\nu k)]^2 < 1 \tag{15}$$

Without acceleration the maximum time step for which the iteration will converge is, therefore, limited.

The success of the application of the acceleration parameters optimized for the solution of the nonlinear equation alone to the simultaneous solution was demonstrated by computer experimentation with both the accelerated [γ given by Eq. (12), $\sigma = 0$] and the unaccelerated ($\gamma = 1$, $\sigma = 0$) solutions. The accelerated solution requires only about 5% of the iterations required by the unaccelerated solution. Since the computer run time is directly proportional to the number of iterations, the accelerated solution can be run in only 5% of the time required by the unaccelerated solution. The conclusion of convergence of the accelerated solution for time steps so large that the unaccelerated solution diverges has also been verified by computer runs, and no divergence of the accelerated solution has yet been found for any time step.

In relation to the question of how closely the convergence properties of the simultaneous solution are approximated by those of the vorticity equation alone, Fig. 1 is presented. This figure shows the results of actual computer runs made with the unaccelerated solution, for which the convergence criteria are given by Eq. (15). The points on this figure represent velocities ranging from 1 fps to 200 fps, viscosities from 0.00016 ft²/sec to 0.016 ft²/sec, and cell sizes from 0.00052 ft to 0.0052 ft. The theoretical boundary between convergence and divergence obtained for the vorticity equation alone is clearly an excellent approximation to the boundary for the simultaneous solution. This adds credence to the assumption that the optimum acceleration parameters for the solution of nonlinear vorticity equation alone are very nearly optimum for the simultaneous solution as well.

The success of this acceleration method, in which the optimum values of two acceleration parameters are determined for the solution of the nonlinear equation alone and then applied to the simultaneous solution, should serve as a guide to the use of a similar technique for other such systems of equations.

References

[1] Thompson, J. F., "Numerical Solution of the Incompressible, Two-Dimensional, Time-Dependent Navier-Stokes Equations for a Body Oscillating in Pitch in a Moving Fluid," Research Rept. 86, 1968, Dept. of Aerophysics and Aerospace Engineering, Mississippi State Univ., State College, Miss.

[2] Thompson, J. F., "Computer Experimentation with an Implicit Numerical Solution of the Navier-Stokes Equations for an Oscillating Body," AIAA Paper 69-185, New York, 1969.

[3] Isaacson, E. K. and Keller, H. B., *Analysis of Numerical Methods*, Wiley, New York, 1966, Chaps. 2 and 9.